RSC Advances

PAPER

View Article Online
View Journal | View Issue

Cite this: *RSC Adv.*, 2023, **13**, 34618

A modified selective optical sensor for selenium determination based on incorporating xylenol orange in a poly(vinyl chloride) membrane

Abeer M. E. Hassan,[a] Reem F. Alshehri,[b] Salah M. El-Bahy,[c] Alaa S. Amin *[d] and Mai Aish[e]

A novel optical sensor has been developed to measure selenium ions. The sensor membrane was created by mixing xylenol orange (XO) and sodium tetraphenylborate (NaTPB) with a plasticized poly(vinyl chloride) membrane that contained *o*-nitrophenyl octyl ether (*o*-NPOE) as a plasticizer. XO was previously established for use in a colorimeter to measure selenium in water and other media. At pH 6.6, the color of the detecting membrane changed from orange to pink when in contact with Se^{4+} ions. Various variables affecting the uptake efficiency were evaluated and optimized. Under optimum conditions (*i.e.*, 30% PVC, 60% *o*-NPOE, and 5.0% of both XO and NaTPB for 5.0 min as the response time), the proposed sensor displayed a linear range 10–175 ng mL^{-1} with the detection and quantification limits of 3.0 and 10 ng mL^{-1}, respectively. Also, the precision (RSD%) was better than 2.2% for six replicate determinations of 100 ng mL^{-1} Se^{4+} in various membranes. For the detection of Se^{4+}, the selectivity of the sensor membrane was investigated for a number of possible interfering inorganic cations, but no appreciable interference was found. With the use of a 0.3 M HCl solution, the sensor was successfully restored, and the response that may have been reversible and reproducible exhibited an RSD% of less than 2.0%. The sensor has been successfully used to analyze Se^{4+} ions in environmental and biological materials.

Received 5th August 2023
Accepted 23rd October 2023

DOI: 10.1039/d3ra05308c

rsc.li/rsc-advances

Introduction

Selenium (Se) is a significant microelement that has a variety of beneficial impacts on diseases and human health. As the levels of Se are incredibly variable across different populations and areas, it is crucial to regulate the status and intake of Se for specific populations. Selenium is one of the trace minerals needed for proper functioning of the body. To maintain homeostasis, human body cells require the right nutrients. Micronutrients, including vitamins, antioxidants, and trace minerals, are essential for numerous regenerative processes, controlling oxidative stress, and establishing immunity against infections.[1]

Selenium is widely distributed in nature in relatively small concentrations in rocks, plants, coal, and other fossil fuels. It exists in environmental samples and living organisms because of the catalytic effects of its compounds in metabolism.[2] Owing to its antioxidant properties and the presence of selenoproteins, selenium is a vital trace element for all living organisms.[3] Selenium has to be present in relatively small amounts for maintaining human and animal health, but in excessive concentrations, it could be hazardous. The organic and inorganic forms of selenium as well as its oxidation configuration are poisonous in nature. In natural waters, the inorganic forms of selenium are more toxic than organic forms, and selenite Se(IV) is more toxic than selenate Se(VI).[4,5]

The World Health Organization (WHO) has set a limit for the selenium concentration in drinking water at 40 ng mL^{-1}.[6,7] While the European Union (EU) and the U.S. Environmental Protection Agency (EPA) have set the limit levels of 50 ng mL^{-1} and 10 ng mL^{-1}, respectively.[8,9] The Se speciation analysis in water becomes difficult due to the need for very sensitive and precise analytical techniques.

Selenium(IV) fractionation issues in soils with plenty of organic matter have received much attention.[10] One of the many physiological tasks performed by selenium(IV) is the protection of cell membranes against oxidative damage. Severe exposure to elemental selenium and selenium oxides can cause a variety of ailments, including bronchitis, stomach aches, coughing, and irritation of the respiratory tract. When selenium levels in the body are above optimal levels, the neurological system is

[a]*Chemistry Department, Faculty of Pharmacy, October 6th University, October, Egypt*
[b]*Chemistry Department, Faculty of Science, Taibah University, Kingdom of Saudi Arabia*
[c]*Chemistry Department, Turabah University College, Taif University, P.O. Box 11099, Taif 21944, Saudi Arabia*
[d]*Chemistry Department, Faculty of Science, Benha University, Benha, Egypt. E-mail: asamin2005@hotmail.com*
[e]*Chemistry Department, Faculty of Science, Port Said University, Port Said, Egypt*

affected. Se(IV) has been discovered to possess anticancer properties. There is growing evidence that selenium is crucial for both human and animal reproduction and growth.[11]

Selenium is considered to be an economically critical mineral in some countries. A low-cost, portable sensor could be useful during the processing of Se (for example, for semiconductors) and for downstream process monitoring. Se speciation in food is crucial for a better understanding of the detection of this metalloid, mainly because selenium absorption has been found to be higher in organic molecules. The low concentration of each species to be identified and the intricacy of the matrix are factors in many selenium speciation analysis issues.[12,13]

Various instrumental analytical techniques such as atomic absorption spectroscopy (AAS),[14–17] atomic fluorescence spectroscopy (AFS),[18] hydride generation atomic fluorescence spectrometry (HGAFS),[19] electrothermal atomic absorption spectrometry (ETAAS),[20] inductively coupled plasma optical emission spectrometry (ICP-OES),[21] hydride generation system and atomic fluorescence spectrometer (HG-AFS),[22] hydride generation atomic fluorescence spectrometer (HG-AFS),[23] integrated coupled plasma mass spectroscopy,[24] inductively coupled plasma mass spectrometry (ICP-MS),[25,26] spectrofluorimetry,[27,28] and stripping voltammetry[29] were used for the determination of selenium in different water, food, and environmental samples. A comprehensive evaluation of these advanced instrumental approaches includes disadvantages related to these techniques, such as expensive investment costs, significant electricity consumption during continuous analysis, the requirement for frequent maintenance of these instruments, and laborious analytical methodology. However, the majority of these methods are complex, relatively costly, time-consuming, and difficult to implement. This prompted the development of a novel and easily deployable optical sensor for the detection of selenate Se(VI). The optical technique has the ability to detect specific oxidation states compared to AAS, and ICP-MS is included.

Spectrophotometry is more accessible, quicker, and less expensive. There are numerous reagents available for selenium spectrophotometric measurement. The spectrophotometric methods for the determination of selenium used J-acid,[30] Leuco crystal violet,[31] resazurin,[32] sodium salt of hexamethyleneimine carbodithioate,[33] 1-naphthylamine-7-sulphonic acid[34] and variamine blue,[35] which have several disadvantages. However, these procedures can only yield the total Se level or are not accurately reliable for detecting ultra-trace Se^{4+}. As a result, preliminary species preconcentration is needed before detection using the above techniques. Additionally, they can offer the required sensitivity and selectivity for environmental checking. However, it lacks selectivity and is hampered by interferences from mutual anions and cations. Consequently, establishing rapid, simple, and effective methods for selenium monitoring at trace levels in water, food, environmental, and biological samples is crucial.

Recently, there has been a focus on the development of chemical methods that reduce the use of compounds that could endanger human health and cause environmental contamination. An alternative strategy is recommended in order to reduce the amount of reagent needed. In the past three decades, interest in the development of optical chemical sensors—also known as optodes or optrodes—as viable substitutes for electrochemical sensors has increased.[36] These sensors have lower detection limits and high sensitivity.[37] Additionally, they may benefit from spectrum characteristics related to the analyte or analyte-specific indication.[38] Furthermore, they are not impacted by electrical noise and do not require internal or external reference devices and extended preconditioning times.[39] The advantages of optical sensor methodology have attracted the attention of the scientific community, as they allow the development of low-cost or cost-competitive systems with faster response times and a wider nano-concentration range and low detection and quantification limits compared with conventional technologies,[14–29,36–39] in addition to the ability to detect specific oxidation states compared to the AAS and ICP-MS methods.[14–26]

The membrane optode matrix is chosen based on analyte permeability, good mechanical properties, plasticizability, affordability, ease of miniaturization and remote sensing, suitability for immobilizing the chromophore and extractant, and minimal sample manipulation.[40–42] Polyvinyl chlorides are the most often utilized polymers in optical sensors. For many applications, they compare favorably with sol–gel matrices and have several advantageous characteristics. The polymers are most frequently utilized in sensors with visible spectrophotometric detections due to their transparency.[43] Numerous sensors have been described in trace analyses of different analytes, including metal ions.[44–49]

Yellow amorphous xylenol orange is easily soluble in conventional organic solvents. Our research team previously employed this reagent for colorimetric tests to examine how selenium interacts with it.[50] The ultimate goal of the current work is to successfully incorporate XO into plasticized PVC film and develop a novel optical sensor with excellent sensitivity and selectivity for the quick measurement of Se^{4+} ions in environmental and biological samples.

Experimental

Reagents

All the chemicals were of analytical grade. Xylenol orange was used without further purification from Sigma (St. Louis, MO, USA). High molecular weight poly(vinyl chloride) (PVC), dioctyl adipate (DOA), dioctyl sebacate (DOS), tributylphosphate (TBP), dibutyl phthalate (DBP), *ortho*-nitrophenyl octyl ether (*o*-NPOE), sodium tetraphenylborate (NaTPB), and tetrahydrofurane (THF), Na2EDTA were from Fluka (Buchs, Switzerland) or Merck (Darmstadt, Germany) Chemical Companies. Universal buffer solutions of pH 2.75–10.63 were prepared as described earlier.[51]

Selenium stock solutions of 5×10^{-3} M were prepared by dissolving an appropriate weight of sodium selenite obtained from BDH Chemical Company (Poole, UK) in the least amount of bidistilled water and completing the volume in a 50 mL measuring flask. Working solutions were obtained by suitable dilution of the stock solution with bidistilled water.

Instrumentation

An Orion research model 601 A/digital ionalyzer pH meter was accomplished for examining the pH of solutions. Electrothermal atomic absorption spectrometry (PerkinElmer Analysis 700 model, Norwalk, CT, USA) was used in this investigation. Selenium EDL lamp was used at 200 mA current, 196.0 nm wavelength, and 2.0 nm spectral band pass. Selenium measurements were carried out as peak area. Operating conditions of selenium in a graphite furnace were adjusted according to manufacturers. Drying, ashing, and atomization temperatures were optimized before analysis. Argon was used at 250 mL min^{-1} flow rate. A Hamilton syringe (10 μL) was performed to transport minor Se^{4+} ion volumes into the cell. The sensor thickness was acquired by a digital microscope (Ray Vision Y 103) that was coupled with a video camera (JVC TK-C 751 EG) and a digital micrometer (Mitutoy, Japan) with an accuracy of ±0.001 mm. UV-vis spectrophotometer model V 53 from JASCO (Tokyo, Japan) was attained for recording the spectra and the absorbance assessments. The absorbance assessments were achieved inside a quartz cuvette by mounting the samples of optical membrane sensors (3.0 cm × 1.0 cm). The absorbance assessments of the optical membrane sensor samples were established with respect to air and a blank sensor sample.

Membrane preparation

The membrane has the right quantities of active ingredients. In a glass vial, 3.0 mL THF was used to dissolve 24 mg of PVC (30%), 48 mg of *o*-NPOE (60.0%), 4.0 mg of XO (5.0%), and 4.0 mg of NaTPB (5.0%). Instantaneously, the mixture was vigorously mixed to attain total homogeneity. The spin-on apparatus was used to spin a glass plate (1 mm × 9 mm × 50 mm), which had been thoroughly cleaned with pure THF to remove any organic contaminants. 90 μL of the aforementioned solution was injected into the glass plate. The membrane was placed in ambient air and spun for 30 s at 600 revolutions per minute before being left to dry for 10 min. Furthermore, the thickness of the PIM was assessed using a digital microscope (Ray Vision Y 103) that was connected to a video camera (JVC TK-C 751 EG). Control membranes were prepared in the same manner. Nevertheless, D2EHPA and CPAHPD were exceptional from the membrane solution. Control membranes were prepared in the same manner. Nevertheless, XO was not presented in the membrane solution. In order to construct the control optical sensor, which is made up of PVC and *o*-NPOE, 24 mg of PVC and 48 mg of *o*-NPOE were dissolved in 3.0 mL of THF. The mixture was stirred for 10 min, poured into a 9.0 cm diameter flat-bottomed Petri dish, and left to evaporate for two days.

Colorimetric procedure

The sensing membrane was placed in a 1.0 cm quartz cell mounted in the spectrophotometer that was already filled with 2.5 mL of the buffer solution of pH 6.6 containing various quantities of Se^{4+}, and it was vigorously stirred for 5.0 min. At 585 nm, the net absorbance of the sensor was determined in comparison to a blank membrane. The blank membrane was defined as a glass-supported membrane that was put in the test solution without Se^{4+} ions. A freshly made sensor membrane was used for every measurement. The absorbance of the samples were examined at 585 nm.

Determination of total Se and Se(VI) species

The determination of total inorganic Se needed a pre-reduction step since the absorption band was produced by a selective radical cation reaction between Se(IV) species and XO. A volume of 3.0 mL of concentrated HCl was added to 10 mL of the sample, and the mixture was heated on a hot plate at 100 °C for at least 30 min to completely reduce Se(VI) to Se(IV). The process for determining total inorganic selenium was then carried out using the reduced samples after they had been allowed to cool at a temperature of 25 ± 2 °C. Finally, the concentration of Se(VI) was calculated by subtracting Se(IV) from total Se.

Interference studies

Standard solutions including 100 ng mL of Fe(III) and 2.0 mg mL^{-1} of one of the following base metal ions frequently found in water samples, Ca(II), Mg(II), Al(III), Cu(II), Pb(II), Co(II), Ni(II), Cd(II), Fe(II), Pd(II), Cr(III), Te(IV), Cr(VI) and Zn(II), were prepared. The solutions were examined by the newly established membrane for this study.

Water sample collection

All sampling materials were washed overnight with a 10% (v/v) HNO_3 solution, rinsed with ultrapure water, and finally, three times with the sample prior to collection. For tap water samples, domestic water was left to run for 20 min, after which a volume of approximately 500 mL was collected in an HDPE bottle. Clean HDPE bottles were used to collect samples of sea, rain, and subsurface water; 500 mL of each type of sample was taken at a depth of 5.0 cm. Sample aliquots were immediately filtered through 0.22 μm pore size PTFE membrane filters (Millipore Corporation) and stored at 4 °C. Sand residues present in seawater were separated by centrifugation prior to filtration. In the Egyptian city of Port Said, seawater was collected. In Benha city (Egypt), samples of rain were taken during a rainstorm, while in El-Madina city (Saudi Arabia), samples of underground water were taken from a well. After neutralization with NH_4OH and completion with buffer pH 6.6, the cooled samples were transferred to a 10 mL measuring flask, mixed thoroughly, and then subjected to the indicated sensor and FAAS procedures for analysis.

Application to food and beverage samples

CS-M-3 mushroom (Boletus edulis) and NIST SRM 1946 fish tissue (100 mg), canned fish, cultivated mushroom, black tea, green tea, coffee, egg, honey, onion, garlic, cow meat, chicken meat, salami, cheese, cabbage, potato, boiled wheat, canned tomato (500 mg), mixed fruit juice and ice tea (1.0 mL) were digested with 6.0 mL HNO_3 (65%) and 2.0 mL H_2O_2 (30%) in

a Milestone Ethos D model closed vessel microwave digestion system according to a reported procedure[52] and diluted to 50 mL with deionized water. In the same manner, and omitting the sample, a blank digestion was also created. On samples that had been digested, the optimized procedure previously described was used. Additionally, ETAAS was used to determine the selenium content.

Determination of selenium in soil sample

A known weight of selenium was mixed with 20 g of the soil sample, fused with 1 : 1 sodium carbonate and potassium nitrate mixture in a nickel crucible and extracted with water. The filtrate of the extract was treated with 20 mL of 10 M hydrochloric acid and then heated to expel chlorine and oxides of nitrogen. For the solution to have an appropriate concentration of selenium, the solution was further diluted with water. To remove the iron present in the soil, a portion of the stock solution was run through the cation exchange resin. Utilizing the sensor mentioned above and using the conventional addition method, the selenium contents were determined.

Determination of Se in human hair

A known amount of human hair was digested with HCl–HNO_3 (3 + 2 v/v; 10 mL) for 10 min. According to the above-described methodology, the solution was cooled, neutralized with diluted NaOH solution, and then analyzed for Se concentration.

Determination of Se in a cosmetic sample

A known weight of a cosmetic sample (lipstick) was dissolved in alcohol to extract any organic material. The residue was gently heated with concentrated HNO_3 (10 mL) for 10 min, and the contents were cooled and then boiled with HCl (10 mL) for 10 min to convert Se(VI) to Se(IV). The sample residue was cooled and then treated with 0.5 M H_2SO_4, 5.0 mL of diluted NaOH solution, neutralization, and bidistilled water dilution to a specified volume (50 mL). The sensor technique for Se was used to analyze the resultant solution.

Results and discussion

Preliminary investigations

According to the previous study,[50] at a pH 6.6, the main species of XO was presented in the solution as L^{2-} that forms a colored radical cation with Se^{4+} and Te^{4+}. It was found that selenium may be determined colorimetrically by optimizing the fabrication of a sensor by including XO and NaTPB in a plasticized PVC membrane containing *o*-NPOE, whereas Te^{4+} radical cation is not created. When Se^{4+} ions diffused into the membrane, it formed radical cations with XO, so the membrane color changed from orange to pink. Fig. 1 shows the absorption spectra of the blank and XO sensors in various concentrations of Se^{4+}.

A schematic showing the sensing moiety and its expected interaction with Se(IV) is shown in Scheme 1.

As can be seen, the membrane spectrum without Se^{4+} ions exhibits a maximum absorbance at $\lambda = 428$ nm, whereas the membrane spectrum with Se^{4+} ions exhibits a maximum absorbance at 585 nm. Comparing the blank and the radical cation spectra of the sensor (Fig. 1) with those in solution,[50] it was observed that the absorbance maxima of both immobilized reagent and radical cation had a bathochromic shift. These results imply that the immobilized reagent's structural conformation is more planar than that of its solution equivalent.[53] The maximal absorbance wavelengths of the membrane are shown at 585 nm in the current work, where Se^{4+} reacts with XO in the sensor membrane. Because of its high selectivity and sensitivity at this maximum, this wavelength was chosen for future studies. It was essential to elucidate the influence of all factors that can possibly affect the prepared sensor.

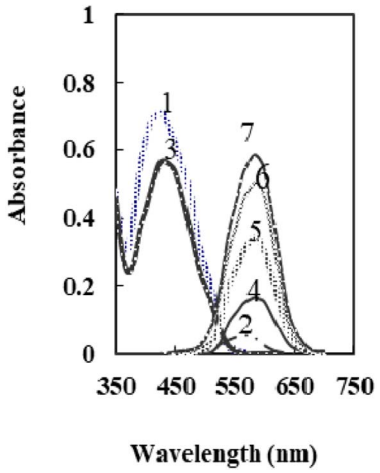

Fig. 1 The absorption spectra of 1: XO in solution, 2: XO-Se in solution, 3: XO sensor, and 4–7: XO-Se sensor at 50, 100, 150, and 175 ng mL^{-1}.

Optimization of the method

To take full advantages of the sensor, amounts of the sensor ingredients and reaction conditions should be optimized. In the one-at-a-time optimization procedure, the absorbance of the membrane in the presence of 100 ng mL^{-1} Se^{4+} at 585 nm was used as the analytical signal.

Effect of membrane composition

The different components utilized in each sensor, such as the base matrix, solvent mediator, ionophore, and the essential

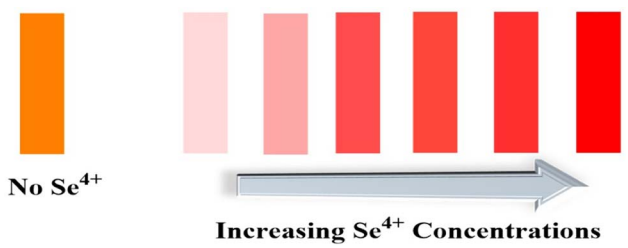

Scheme 1 The sensing moiety of the membrane sensor and its reactivity in the presence of different [Se^{4+}].

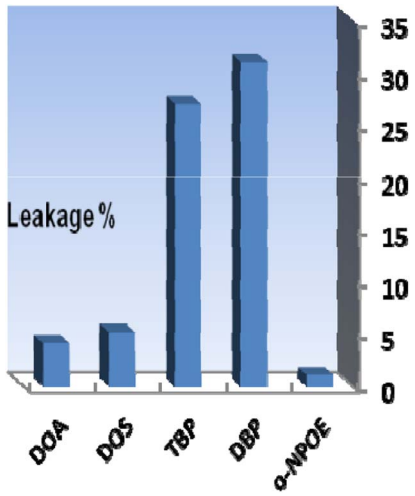

Fig. 2 The effect of plasticizer nature on the membrane leakage% after 30 min. Conditions: $[Se^{4+}] = 100$ ng mL^{-1}, $T = 25$ °C; the membrane layer contained 24 mg of PVC, 48 mg of each plasticizer, and 4.0 mg of XO.

additive used in the membrane construction, have a major impact on the response characteristics and working concentration range. As a result, choosing the sensor matrix is crucial. It was observed that high molecular weight PVC could be used as the membrane base. This selection was due to several parameters, such as appropriate transmittance, suitable immobilization of XO as the reagent without any leakage, good mechanical stability, and reliable permeability to Se^{4+} ions.

Solvent mediators (plasticizers) must be physically compatible with the polymer utilized to prepare the sensor membrane to produce a homogeneous organic phase. As potential plasticizers, several solvents, including DOA, DOS, TBP, DBP, and *o*-NPOE, were evaluated in this study. As seen in Fig. 2, the membranes containing DOA or DOS had improper physical properties, indicating that these membrane solvents did not cause a suitable signal for the proposed membrane sensor. Also, as shown in Fig. 2, TBP and DBP plasticizers showed good sensitivity, but membranes containing these plasticizers showed reagent leakage at short times. The membrane containing *o*-NPOE was the appropriate selection with respect to high sensitivity and minimum leakage of XO from the membrane. As shown in Table 1, the membrane sensors with a weight ratio of *o*-NPOE to PVC of 2.0 provided better absorbances. Thus, 48 mg *o*-NPOE (60.0%) was selected as an optimum value.

XO performs two different functions in the proposed sensor membrane: chromoionophore and ionophore. Optimizing its concentration in the membrane composition is, therefore, necessary. The effect of different amounts of XO on the membrane response is shown in Table 1. As can be seen, the absorbance rose with increasing XO concentrations up to 4.0 mg and fell with higher concentrations caused by membrane leakages. Therefore, the optimal value of 4.0 mg XO (5.0%) was chosen.

The addition of an anionic additive, such as NaTPB, promotes the ion–exchange equilibrium by allowing for the entire mass transfer of Se^{4+} ions into the membrane and by reducing response time.[54] Thus, in the subsequent studies, the effect of NaTPB (4.0 mg) as an anionic additive was tested on the membrane properties with different plasticizers. As can be seen in Fig. 3, the presence of NaTPB caused an increase in the sensor responses and reagent leakages from all membranes. It is clear that utilizing a sensor with *o*-NPOE allowed for the

Table 1 The effect of membrane composition on the absorbance of the proposed sensor membrane

Sensor	PVC (mg)	*o*-NPOE (mg)	XO (mg)	NaTPB (mg)	Response time (min)	Absorbance[a] (585 nm)
1	24	40	4	4	5	0.336
2	24	44	4	4	5	0.421
3	24	48	4	4	5	0.501
4	24	52	4	4	5	0.442
5	24	56	4	4	5	0.271
6	24	48	1	4	5	0.231
7	24	48	2	4	5	0.384
8	24	48	3	4	5	0.453
9	24	48	4	4	5	0.502
10	24	48	5	4	5	0.453
11	24	48	4	1	5	0.237
12	24	48	4	2	5	0.308
13	24	48	4	3	5	0.436
14	24	48	4	4	5	0.500
15	24	48	4	5	5	0.417
16	24	48	4	4	1	0.269
17	24	48	4	4	3	0.462
18	24	48	4	4	5	0.500
19	24	48	4	4	7	0.499
20	24	48	4	4	10	0.498

[a] Mean absorbance ($n = 4$) of every parameter is recorded from four solutions of 100 ng mL^{-1} Se^{4+} (pH 6.6).

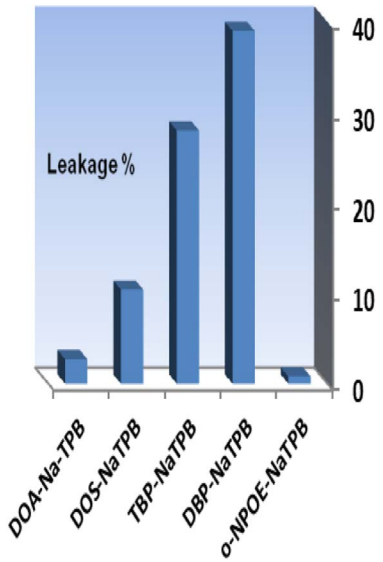

Fig. 3 The effect of the anionic additive with different plasticizers on the membrane leakage% after 5.0 min. Conditions: [Se^{4+}] = 100 ng mL^{-1} and T = 25 °C; the membrane layer contained 24 mg of PVC, 48 mg of each plasticizer, and 4.0 mg of XO.

greatest achievable response and the least amount of XO leaking from the membrane. The amount of NaTPB was investigated in the range of 1.0–5.0 mg. The results are given in Table 1. It is shown that the highest absorbance is recorded by using 4.0 mg of NaTPB. Lower concentrations saw a drop in associated absorbances due to less mass transfer of Se^{4+}, while higher concentrations saw a decrease due to XO leakage. Therefore, 4.0 mg NaTPB (5.0%) was selected as the optimal amount in the membrane composition.

Effect of pH

The effect of pH variation on the sensor response was investigated in the range of 2.65–10.50. At pH 6.6, optode absorbance reaches its peak (Fig. 4). The low concentration of chromoionophore in the membrane, which serves as a potential binding site and prevents Se^{4+} ions from completely permeating, accounts for a drop in the metal uptake efficiency at pH < 6.6. At pH > 7.0, hydrolysis of Se^{4+} ions occurs, and hydroxide species probably caused the incomplete diffusion of Se^{4+} ions into the membrane. Therefore, a buffer of pH 6.6 was chosen in all experiments.

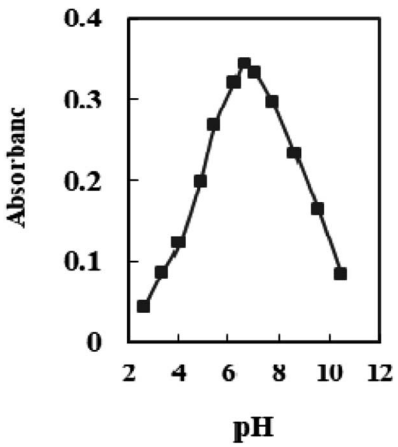

Fig. 4 The absorbance of the sensor in solutions containing 100 ng mL^{-1} Se^{4+} at different pH values.

Effect of response time

The definition of response time for sensors is the time it takes for metal ions to diffuse from the solution into the membrane (the slowest phase in the radical cation process). The effect of this parameter on the sensor response was investigated in the range of 1.0–10 min. As seen in Table 1, a time interval of at least 5.0 min is required for quantitative uptake at 25 ± 2.0 °C (Fig. 5). It was found that response time has a reverse relation toward initial Se^{4+} ion concentrations and the response time significantly increased from 3.0 min to 5.0 min by raising the Se^{4+} ion concentration from 50–150 ng mL^{-1}. In general, the response time is lower in concentrated solutions than in dilute solutions (Table 2).

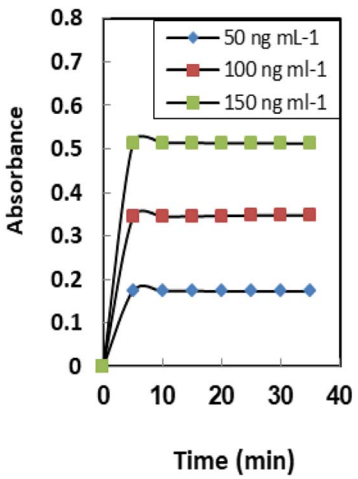

Fig. 5 The response time of the sensor membranes for different concentrations of Se^{4+}. Conditions: pH 6.6 and T = 25 °C; the membrane layer contained 24 mg of PVC, 48 mg *o*-NPOE, and 4.0 mg of both XO and NaTPB.

Table 2 The tolerance ratio (TR = ion/Se^{4+} mass ratio) for various interfering ions in the determination of 100 ng mL^{-1} of Se^{4+}

Ion	TR	Ion	TR
Na^+, K^+, Li^+	12 500	Al^{3+}, Fe^{3+}, CO_3^{2-}	4000
Ca^{2+}, Mg^{2+}, acetate	11 000	Fe^{2+}, NH_2OH	3500
Ag+, Cu^{2+}, NO_3^-	1000	Cd^{2+}, Ni^{2+}, SO_4^{2-}	3000
Sr^{2+}, Ba^{2+}, $S_2O_3^{2-}$	8500	Hg^{2+}, Co^{2+}, oxalate	2750
Ge^{4+}, Ti^{4+}, citrate	7000	Cu^{2+}, Sn^{2+}, HCO_3^{2-}	2500
Bi^{2+}, Sn^{2+}, Mn^{2+}	6000	Pb^{2+}, Pd^{2+}, SCN^-	2000
Zr^{4+}, Cr^{6+}, succinate	5500	Au^{3+}, La^{3+}, Cr^{3+}	1750
Mo^{6+}, W^{6+}, Br^-	5000	Se^{6+}, Te^{6+}, NH_4^+	1500
Th^{4+}, UO_2^{2+}, $B_4O_7^{2-}$	4500	Te^{4+}	120

Effect of stirring

Stirring the Se^{4+} solution has a large influence on the response of the formed sensor. About tenfold enhancement was achieved when the Se^{4+} solution was stirred compared to the non-stirred solution. This observation can be explained by the movement of Se^{4+}ions towards the immobilized XO. The Se^{4+} ion diffusion through the membrane to the XO has been sped up by the stirring procedure, which has also sped up the Se^{4+} ion-XO reaction. Regarding the non-stirring procedure, the concentration gradient is the only factor that influences the diffusion of Se^{4+} ions across the membrane.[55]

The average thickness of the prepared sensor membrane was established to be 31 ± 2 mm. The thickness of the membrane was assessed during the experiments by a digital microscope (Ray Vision Y 103) connected to a video camera (JVC TK-C 751EG). This thickness of the membrane achieved is appropriate for ion mobility for the reaction of Se^{4+} with XO. This is because the membrane is not too thick (>100 mm) and not too thin (<5 mm) and is reasonable to be applied as a transducer for sensor membrane depending on the co-extraction principle.[56]

Membrane properties

The properties of the sensor membrane were measured by recording absorbance changes at 585 nm from individual solutions of 50, 100, and 150 ng mL^{-1} Se^{4+}. It is obvious from Fig. 5 that, in all three cases, the sensors reached 95% response after 5.0 min of stirring. The stability of membranes was tested for 3.0 h, and during this period, the mean difference of absorbances for the mentioned solutions was ±0.011. The membrane responses were stable for 15 days in the air.

One of the key features of sensor membranes is their ability for regeneration, which enables repeated use of the tested sensor and much lower reagent use. Given that the membrane is not entirely reversible on its own, it can be regenerated using an appropriate stripping reagent. The time it takes for the sensor to return to its steady state baseline after being loaded with the regenerating solution is how the regeneration time is measured. As stripping reagents, a number of substances, including HCl, H_2SO_4, HNO_3, KBr, KI, and KSCN, were studied. Complete regeneration with HNO_3 and H_2SO_4 solutions was relatively long, and the sensors in contact with these solutions only recovered 80% of their initial absorbance after 10 min. Although all the other reagents were efficient for regenerating the sensor membranes, the shortest regeneration time was achieved with the HCl solution. The effect of the concentration of the stripping reagent was also illustrated. The best results were observed with 0.3 M HCl solution, although lower concentrations of down to 0.1 M can also be applied with increased regeneration times. The mechanism of regeneration is represented as $SeCl_4$ is rapidly formed while using 0.3 M HCl rather than 0.1 M HCl due to the slow formation of $SeCl_2$. The proposed mechanism for the interaction between the XO sensor and the Se^{4+} ions and its complexation and regeneration is depicted in Scheme 2.

The regeneration times of the sensors after contact with the 50, 100, 150 ng mL^{-1} Se^{4+} solutions were 40, 40, and 50 s,

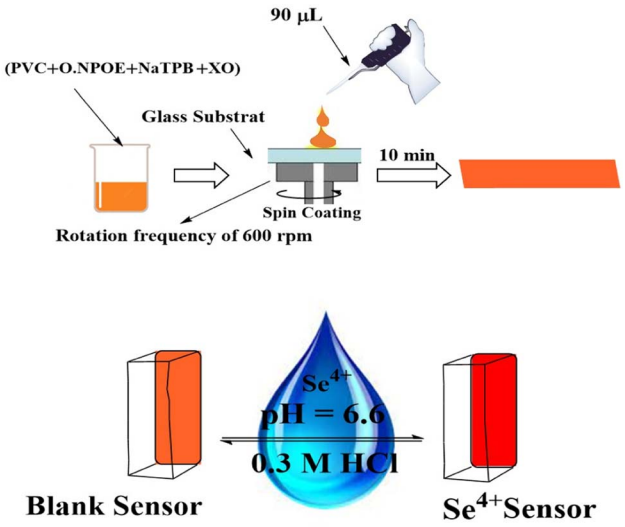

Scheme 2 Schematic representation for the preparation, complexation, and regeneration of the formed optical sensor.

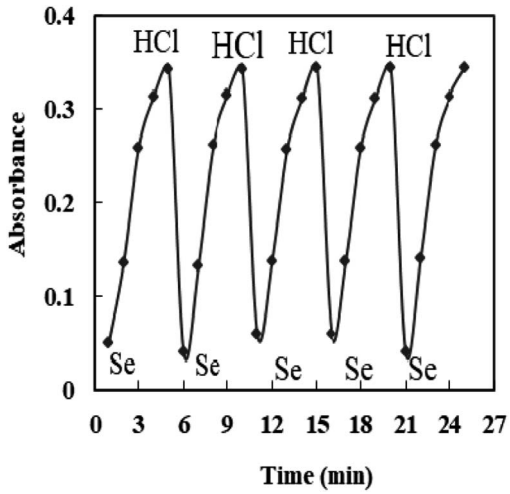

Fig. 6 The reversibility of the sensor exposed to 100 ng mL^{-1} Se^{4+} and 0.3 M HCl.

respectively, when 0.3 M HCl was used as the stripping reagent (Fig. 6). It should be mentioned that there is no requirement for the regeneration step if the measurement is brought from lower to higher Se^{4+} ion levels.

Interference

The relative sensitivity of the sensor membrane to the principal ion over concurrent ions in the solution is one of its most significant characteristics.[57] The cations and anions that could interact with the optode's ionophore or species that might react with Se^{4+} ions and reduce the diffusion and migration efficiency are the interferences. The concentration that results in an error of more than ±5.0% in the absorbance, known as the tolerance limit for Se^{4+} ions, was chosen as the tolerance limit.[58,59] In this regard, the absorbance of the sensor before and after the

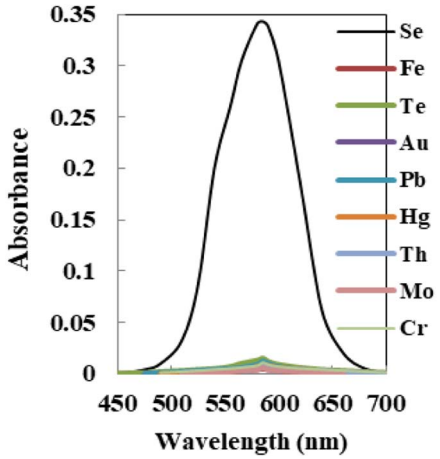

Fig. 7 The absorption spectra of the sensor with each potential interfering metal tested on 100 ng mL^{-1} of Se^{4+} using the membrane.

addition of a fixed amount of interference ions into 100 ng mL^{-1} of Se^{4+} ion solution was recorded, as shown in Fig. 7, and results are given in Table 3. The results confirmed that the sensor membrane exhibited excellent selectivity toward Se^{4+} ions with respect to the other coexisting interference ions at $\lambda_{max} = 585$ nm except for Te^{4+} ions, which at concentrations of >120 fold mass ratios do not interfere. Taking into account that the maximum acceptable concentration of those species in water, food, and biological samples was lower than the tolerance limit found, the procedure could be useful for Se determination.

Speciation studies

The suggested optical sensor was examined as a promising candidate for the Se^{4+}/Se^{6+} speciation due to its excellent selectivity for Se^{4+}. In solutions including various amounts of Se^{4+} and Se^{6+} ions, the concentration of Se^{4+} ion can be assessed under optimal experimental circumstances with the offered optode. Then, the total concentration of selenium can also be detected in the same way after the reduction of Se^{6+} to Se^{4+}. Finally, the Se^{6+} ion concentration is assessed by subtracting the amount of Se^{4+} from the total amount of selenium.

To make a comparison, ETAAS also evaluated the overall amount of selenium. Table 3 shows the outcomes for the

Table 4 The analytical characteristics of the offered sensor membrane

Parameters	Proposed sensor
pH	6.6
λ_{max} (nm)	585
Beer's range (ng mL^{-1})	10–175
Ringbom range (ng mL^{-1})	25–160
Molar absorptivity (L mol^{-1} cm^{-1})	7.17×10^7
Detection limit (ng mL^{-1})	3.0
Quantification limit (ng mL^{-1})	10
Reproducibility (RSD%)[a]	2.2
Regression equation	
Slope (ng mL^{-1})	16.4
Intercept	−0.04
Correlation coefficient (r)	0.9980

[a] For six replicate determinations of 100 ng mL^{-1} Se^{4+}.

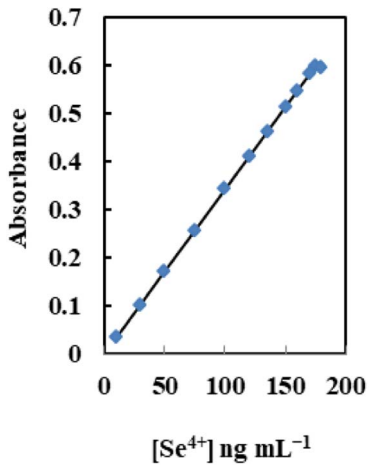

Fig. 8 The dynamic range of the sensor at the optimum conditions for different [Se^{4+}].

selenium speciation at different Se^{4+}/Se^{6+} ratios. Table 3 shows that, within the experimental errors given, the total amounts of selenium measured by the suggested sensor membrane and those identified by the ETAAS technique are in good agreement. Furthermore, in all Se^{4+}/Se^{6+} mixtures checked, the amount of

Table 3 The determination of Se^{4+} and total selenium in different Se^{4+}/Se^{6+} mixtures

		Found by the sensor; ng mL^{-1}		
Sample	[Se^{4+}] and [Se^{6+}]; ng mL^{-1}	[Se^{4+}]	Total SE	Total Se, ETAAS
1	[Se^{4+}] = 50; [Se^{6+}] = 0.0	49.6 ± 0.07	49.6 ± 0.51	50.7 ± 0.25
2	[Se^{4+}] = 50; [Se^{6+}] = 25	49.5 ± 0.12	75.4 ± 0.68	74.4 ± 0.41
3	[Se^{4+}] = 50; [Se^{6+}] = 50	50.7 ± 0.11	99.2 ± 0.74	101.2 ± 0.36
4	[Se^{4+}] = 70; [Se^{6+}] = 70	70.5 ± 0.08	140.8 ± 0.91	138.6 ± 0.29
5	[Se^{4+}] = 80; [Se^{6+}] = 40	80.5 ± 0.09	119.6 ± 0.77	121.2 ± 0.26
6	[Se^{4+}] = 80; [Se^{6+}] = 80	79.4 ± 0.14	158.6 ± 0.83	161.8 ± 0.37
7	[Se^{4+}] = 40; [Se^{6+}] = 80	39.5 ± 0.10	121.4 ± 0.69	118.9 ± 0.28
8	[Se^{4+}] = 60; [Se^{6+}] = 100	60.8 ± 0.15	158.6 ± 0.58	162.4 ± 0.43

Table 5 The comparison of the present method with literature values for selenium determination[a]

Media[a]	Technique	LOD (ng L^{-1})	RSD (%)	Ref.
SPE (Chemically modified mesoporous silica)	ICP-OES	2560	3.84	22
SPE (CTAB modified alkyl silica)	ICP-OES	100	3.6	60
SPE (Modified multi-wall carbon nanotubes)	ICP-MS	16	6.2	61
SPE (GO-TiO_2)	GFAAS	40	9.4	62
SPE (2,6-Diamino-4-phenil-1,3,5-triazine bonded silica gel)	GFAAS	15	<8	63
SPE (Magnetic multi-walled carbon nanotubes)	HGAFS	13	2.3	64
Vortex assisted based liquid–liquid micro extraction (VA-LLME) method	ETAAS	70	4.6	65
oxMWCNTs	ETAAS	30	4	20
MSPME (Polystyrene-*g*-polyoleic acid-*g*-polyethylene glycol *graft* copolymer)	ETAAS	6.60	3.2	66
SPE (Polyvinyl chloride)	HG-ICP-OES	30	5.7	67
Au-coated W-coil atom trap	HG-AAS	21	3.2	68
SPE (Mg–$FeCO_3$ layered double hydroxides loaded cellulose fibre)	HGAFS	11	3.3	69
CHLLME	HGAFS	10	3.8	19
On-line flow injection analysis	Spectrofluorometry	270	2.0	27
2,3-Dichloro-6-(2,7-dihydroxy-naphthylazo)quinoxaline	Spectrophotometry	60	1.2	70
Optical sensor membrane	Colorimetrry	3.0	2.2	This work

[a] MSPME: Magnetic solid phase micro extraction, SPE: solid phase micro extraction, LOD: limit of detection RSD: relative standard deviation, PF: preconcentration factor, CHLLME: continuous homogeneous liquid–liquid microextraction, cxMWCNTs: oxidized multiwall carbon nanotubes.

Table 6 The application of the present method to water and beverage, soil, human hair, and cosmetic samples for the determination of selenium ions

		Found[a] [ng mL^{-1}]				
Samples	Added [ng mL^{-1}]	Sensor	ETAAS	Recovery (%)	*t*-test[b]	*F*-value[b]
Tap water	—	0.40 ± 0.06	0.45 ± 0.85			
	40	40.75 ± 0.08	41.00 ± 0.77	100.87	1.86	
	80	79.60 ± 0.13	81.00 ± 1.05	99.00		3.77
Mineral water	—	0.30 ± 0.07	0.27 ± 1.15			
	50	50.50 ± 0.11	49.80 ± 1.20	100.40	1.67	
	100	99.90 ± 0.18	101.0 ± 0.95	99.60		3.93
Underground water	—	0.65 ± 0.14	0.60 ± 0.85			
	60	60.35 ± 0.09	61.0 ± 1.05	99.50	2.11	
	120	121.0 ± 0.10	120.2 ± 1.30	100.29		4.05
Rain water	—	0.25 ± 0.15	0.25 ± 0.90			
	70	69.90 ± 0.07	70.70 ± 0.80	99.50	1.83	
	140	140.6 ± 0.12	139.5 ± 1.00	100.25		3.93
River water	—	0.55 ± 0.06	0.50 ± 1.10			
	80	80.05 ± 0.08	81.00 ± 1.25	99.94	1.47	
	160	161.3 ± 0.13	159.6 ± 0.75	100.47		3.73
Ice tea	—	1.00 ± 0.08	1.00 ± 1.15	—		
	55	55.25 ± 0.16	57.2 ± 0.95	98.66		4.04
	110	113.2 ± 0.20	108.5 ± 0.85	101.98	1.97	
Mixed fruit juice	—	75.5 ± 0.25	75.0 ± 1.20			
	50	126.5 ± 0.21	124.2 ± 1.45	100.80		3.78
	100	173.7 ± 0.13	177.0 ± 0.95	98.97	2.03	
Fresh cabbage[c]	—	1.12 ± 0.07	1.15 ± 1.05			
	75	77.00 ± 0.11	74.65 ± 1.30	101.16	1.88	
	150	149.7 ± 0.17	153.0 ± 1.55	99.06		3.75
Soil[c]	—	0.25 ± 0.09	0.25 ± 0.75			
	65	65.75 ± 0.14	64.30 ± 1.00	100.77	2.14	
	130	128.8 ± 0.19	131.8 ± 1.35	98.88		4.16
Cosmetic preparation (5.0 g lipstick)	—	253.5 ± 0.04	254.0 ± 1.55			
	100	365.7 ± 0.11	335.8 ± 2.05	103.45	2.04	
	175	415.4 ± 0.13	435.5 ± 1.85	96.90		3.89
	—	225.8 ± 0.15	220.8 ± 1.65			
Human hair (0.5 g)	65	280.5 ± 0.18	300.5 ± 0.19	98.15	1.83	
	130	360.7 ± 0.20	330.4 ± 0.19	101.38		3.65

[a] Mean ± SD. [b] Theoretical values for *t* and *F* values at 95% confidence level for five degrees of freedom are 2.57 and 5.05, respectively. [c] μg kg^{-1}.

both Se^{4+} and Se^{6+} ions present in the initial solutions can be assessed precisely.

Analytical characteristics

Table 4 lists the analytical features of the improved sensor membrane, including the regression equation, linear range (Fig. 8), detection and quantification limits, and selenium determination reproducibility. The limits of detection and quantification, defined as $C_{DL} = 3S_B/m$ and $C_{QL} = 10S_B/m$ (where C_{DL}, C_{QL}, S_B, and m are the limit of detection, the limit of quantification, standard deviation of the blank, and slope of the calibration equation, respectively), were 3.0 and 10 ng mL^{-1}. Additionally, 2.2% was the relative standard deviation (RSD%) for six replicate analyses of 100 ng mL^{-1} Se^{4+} in different membranes. This shows that the produced sensors' responses are repeatable and that the individual measurements did not significantly deviate from one another.

Table 5 presents a comparison between the proposed optode and the other reported techniques recommended in the literature[19,20,22,27,60–69] for the determination of selenium. It is clear that the suggested approach has many benefits, including simplicity, low cost, rapidity, minimal toxicity, and relatively high selectivity. Comparing the given sensor to the reported sophisticated approaches, the linear range and detection limit are excellent; however, a review of the literature reveals that there have been no reports on a sensor membrane with chip reagents for assessing Se^{4+} ions in solutions. Furthermore, the offered method is simple and rapid compared with the reported procedures. Although the results obtained in the proposed sensor were primarily focused on Se^{4+} detection, the proposed sensor may be readily applied for the determination of selenium in real samples without interference from other metal ions.

Validation and application

The proposed sensor was used to measure selenium in actual water samples in order to assess the analytical applicability of the proposed sensor. Six different types of water samples were therefore chosen, including tap, mineral, subterranean, rain, sea, and river water. The results of the proposed methodology are recorded in Table 6. As seen, the mean recoveries for the addition of different concentrations of selenium to water samples are in the range of 98.66–101.98%. Therefore, the proposed sensor membrane can be successfully applied for the determination of Se^{4+} in various water samples.

The developed method was applied to the quantitative determination of traces of selenium in real matrices such as soil and human hair samples, *viz.*, cosmetic preparations. The results of an analysis of the above samples (Table 6) compare favorably with those from the ETAAS method.[20]

The performance of the proposed sensor was assessed using the *t*-value (for accuracy) and *F*-test (for precision) compared with the ETAAS method.[20] The mean values were obtained by a Student's *t*-test and *F*-test at 95% confidence limits for five degrees of freedom.[71] The outcomes demonstrated that the calculated values (Table 6) did not surpass the theoretical values. The advantage of the suggested method over prior ones is that it has a larger range of determination, greater precision, greater stability, and requires less time.

Table 7 The application of the proposed method to microwave digested food samples for the determination of selenium

	Selenium ($\mu g\ kg^{-1}$)[a] ± SD			
Samples	Sensor	ETAAS	*t*-test[b]	*F*-value[c]
Canned tomato	187 ± 0.11	185 ± 1.07	1.27	2.63
Potato	99 ± 0.09	100 ± 0.84	1.53	2.96
Coffee	188 ± 0.16	185 ± 0.88	1.07	2.35
Black tea	284 ± 0.19	280 ± 1.32	1.33	2.75
Green tea	143 ± 0.11	145 ± 1.03	1.48	2.62
Honey	197 ± 0.18	200 ± 0.96	1.22	2.48
Garlic	344 ± 0.20	345 ± 1.24	1.36	2.84
Egg	167 ± 0.14	165 ± 1.13	1.74	3.17
Salami	160 ± 0.10	160 ± 0.79	1.11	2.39
Onion	273 ± 0.24	270 ± 0.92	1.29	2.67
Cultivated mushroom	215 ± 0.12	217 ± 0.69	1.45	2.72
Canned fish	430 ± 0.35	427 ± 0.85	1.67	2.98
Cows meat	226 ± 0.17	230 ± 1.17	1.41	2.56
Boiled wheat	135 ± 0.12	140 ± 0.95	1.63	3.04
Cheese	263 ± 0.22	260 ± 1.28	1.16	2.53
Chicken meat	158 ± 0.13	155 ± 1.05	1.44	2.69

[a] Mean ± SD. [b] Theoretical values for *t*-test at 95% confidence level for five degrees of freedom is 2.57. [c] Theoretical values for *F*-value at 95% confidence level for five degrees of freedom is 5.05.

Various microwave-digested food samples, such as canned tomato, potato, coffee, black tea, green tea, honey, egg, garlic, salami, onion, cultured mushroom, canned fish, cow meat, boiled wheat, cheese, and chicken meat, were also effectively tested using the current method. The results are given in Table 7. These samples contained different matrix media. Selenium levels were determined at $\mu g\ kg^{-1}$ levels in analyzed food samples. The selenium ions found in the analyzed food, beverage, and water samples had levels that were suitable for human consumption. Some food and drink samples can significantly increase selenium consumption.

Conclusions

The suggested sensor membrane, which is based on an optical sensor membrane linked with spectrophotometry, is a low-cost, precise, sensitive, and highly selective method for determining selenium. The suggested method offers a broad dynamic range, trustworthy reproducibility, and good limits of detection and quantification, in addition to being quick and easy. In addition to being quick and simple to use, the proposed sensor also offers a detection limit comparable to previous techniques, according to a comparison of the proposed sensor with previously reported techniques for selenium determination (Table 5). It is crucial to note that this method is being used for the first time and has not previously been mentioned in the literature as being used for selenium speciation and determination. Finally, the selenium in actual environmental and biological samples may be monitored with success using the developed optical sensor membrane.

Author contributions

Abeer Hassan and Reem Alshehri: conceptualization, data curation, investigation, methodology, visualization, validation, writing – original draft, writing – review & editing. Salah El-Bahy and Alaa Amin: conceptualization, methodology, data curation, investigation, supervision, validation, writing – original draft, writing – review & editing. Mai Aish: conceptualization, investigation, methodology, validation, writing - original draft, writing – review & editing.

Conflicts of interest

The authors declare that they have no conflict of interest.

Acknowledgements

The researchers acknowledge the Deanship of Scientific research, Taif University, for funding this work. The authors would like to acknowledge financial support from the Department of Chemistry, Faculty of Science, Taibah, Benha, and Port Said Universities for providing instrumental facilities.

References

1 P. T. Bhattacharya, S. R. Misra and M. Hussain, *Scientifica*, 2016, 5464373.
2 H. Asiabi, Y. Yamini, S. Seidi, M. Shamsayei, M. Safari and F. Rezaei, *Anal. Chim. Acta*, 2016, **922**, 37–47.
3 K. Kocot, R. Leardi, B. Walczak and R. Sitko, *Talanta*, 2015, **134**, 360–365.
4 L. C. Herrero, G. J. Barciela, M. S. García and C. R. M. Peña, *Anal. Chim. Acta*, 2013, **804**, 37–49.
5 M. Tuzen and O. Z. Pekiner, *Food Chem.*, 2015, **188**, 619–624.
6 WHO, *Selenium in drinking-water. Background document for preparation of WHO Guidelines for drinking-water quality*, World Health Organization (WHO/SDE/WSH/03.04/13), Geneva, 2003.
7 WHO, *Guidelines for Drinking-Water Quality*, World Health Organization, 2011.
8 EU, *Directive of the European Parliament and of the Council on the Quality of Water Intended for Human Consumption*, European Commission, 2017.
9 EPA, *National Primary Drinking Water Regulation Table*, U.S. Environmental Protection Agency, U.S.A., 2009.
10 M. Bujdos, J. Kubove and V. Stresko, *Anal. Chim. Acta*, 2000, **408**, 103–109.
11 H. D. Mistry, P. F. Broughton, L. Redman and L. Poston, *Am. J. Obstet. Gynecol.*, 2012, **206**, 21–30.
12 S. Otles, *Methods of Analysis of Food Components and Additives*, CRC Press, 2005.
13 M. B. Melwanki and J. Seetharamappa, *Turk. J. Chem.*, 2000, **24**, 287–291.
14 B. V. Samlafo, P. O. Yeboah and Y. J. Serfor-Armah, *Appl. Sci. Technol.*, 2011, **16**, 1–2.
15 N. Altunay, A. Elik and K. Katin, *J. Food Compos. Anal.*, 2021, **99**, 103871.
16 L. Chirita, E. Covaci, A. Mot, M. Ponta, A. Gandeac and T. Frentiu, *J. Anal. At. Spectrom.*, 2021, **36**, 267–272.
17 B. G. Nieto, J. Gismera, T. Sevilla and J. R. Procopio, *Anal. Chim. Acta*, 2022, **1202**, 339637.
18 M. Llaver, A. L. Chapana and R. G. Wuilloud, *Talanta*, 2021, **222**, 121460.
19 A. Shishov, M. Wieczorek, P. Kościelniak, D. Dudek-Adamska, A. Telk, L. Moskvin and A. Bulatov, *Talanta*, 2018, **181**, 359–365.
20 A. M. Martínez, S. Vázquez, R. Lara, L. D. Martínez and P. Pacheco, *Spectrochim. Acta, Part B*, 2018, **140**, 22–28.
21 M. Murillo, N. Carrio, M. Quintana, G. Sanabria, R. Manuel, L. Duarte and F. Ablan, *J. Trace Elem. Med. Biol.*, 2005, **19**, 23–27.
22 H. Sereshti, Y. E. Heravi, S. Samadi, A. Badiei and N. H. Roodbari, *Food Anal. Methods*, 2013, **6**, 548–558.
23 D. Mazej, I. Falnoga, M. Veber and V. Stibilj, *Talanta*, 2006, **68**, 558–568.
24 J. Pinho, J. Canario, R. Cesario and C. Vale, *Anal. Chim. Acta*, 2005, **551**, 207–212.
25 Y. Yuan, Y. Shao, F. Yang, H. Yu, Y. Zhang and M. Wen, *Spectrochim. Acta, Part B*, 2023, **203**, 106664.
26 Y. Chen, N. Guo, L. Zhang, K. Hu, J. Yang and K. Shi, *J. Radioanal. Nucl. Chem.*, 2023, **332**, 1071–1081.
27 D. G. Santarossa and L. P. Fernández, *Talanta*, 2017, **172**, 31–36.
28 M. Acosta, L. P. Fernandez and M. C. Talio, *J. Fluoresc.*, 2023, **17**, 1–10.
29 P. Devi, R. Jain, A. Thakur, M. Kumar, N. K. Labhsetwar, M. Nayak and P. Kumar, *Trends Anal. Chem.*, 2017, **95**, 69–85.
30 R. Manish, K. N. Ramachandran and V. K. Gupta, *Talanta*, 1994, **41**, 1623–1626.
31 D. Agarwal, G. Sunitha and V. K. Gupta, *J. Indian Chem. Soc.*, 1998, **73**, 151–154.
32 A. Safavi and A. Afkhami, *Anal. Lett.*, 1995, **28**, 1095–1101.
33 M. N. Pathare and A. D. Sawant, *Anal. Lett.*, 1995, **28**, 317–334.
34 K. Pyrzynska, *Anal. Sci.*, 1997, **13**, 629–632.
35 H. D. Revanasiddappa and T. N. Kiran Kumar, *Anal. Sci.*, 2001, **17**, 1309–1312.
36 M. R. Ganjali, M. Hosseini, M. Hariri, F. Faridbod and P. Norouzi, *Sens. Actuators, B*, 2009, **142**, 90–96.
37 W. R. Seitz, in *Optical Ion Sensing Fiber Optic Chemical Sensors Biosensors II*, ed. O. S. Wolfbeis, CRC Press, Bocaraton, FL, 1991, pp. 1–19.
38 M. Shamsipur, M. Sadeghi, K. Alizadeh, H. Sharghi and R. Khalifeh, *Anal. Chim. Acta*, 2008, **630**, 57–66.
39 G. Absalan, M. Asadi, S. Kamran, S. Torabi and L. Sheikhian, *Sens. Actuators, B*, 2010, **147**, 31–36.
40 Y. Kalyan, A. K. Pandey, P. R. Bhagat, R. Acharya, V. Natarajan, G. R. K. Naidu and A. V. R. Reddy, *J. Hazard. Mater.*, 2009, **166**, 377–382.
41 M. R. Ganjali, R. Zare-Dorabei and P. Norouzi, *Sens. Actuators, B*, 2009, **143**, 233–238.
42 Y. Kalyan, A. K. Pandey, G. R. K. Naidu and A. V. R. Reddy, *Spectrochim. Acta, Part A*, 2009, **74**, 1235–1241.

43 S. Rastegarzadeh, N. Pourreza and I. Saeedi, *J. Hazard. Mater.*, 2010, **173**, 110–114.
44 H. H. El-Feky, A. S. Amin and E. M. I. Moustafa, *RSC Adv.*, 2022, **12**, 18431–18440.
45 E. M. I. Moustafa, A. S. Amin and M. A. El-Attar, *Anal. Biochem.*, 2022, **654**, 114835.
46 H. H. El-Feky, S. El-Bahy and A. S. Amin, *Anal. Biochem.*, 2022, **651**, 114720.
47 H. H. El-Feky, A. M. Askar and A. S. Amin, *RSC Adv.*, 2021, **11**, 35300–35310.
48 A. S. Amin, S. El-Bahy and H. H. El-Feky, *Anal. Biochem.*, 2022, **643**, 114579.
49 L. dlC. Coo and I. S. Martinez, *Talanta*, 2004, **64**, 1317–1322.
50 A. S. Amin and M. M. Zareh, *Anal. Lett.*, 1996, **29**, 2177–2189.
51 H. T. S. Britton, *Hydrogen Ions*, Chapman and Hall, London, UK, 4th edn, 1952, p. 1168.
52 A. Naeemullah, M. Tuzen and T. G. Kazi, *J. Ind. Eng. Chem.*, 2018, **57**, 188–192.
53 A. Safavi and M. Bagheri, *Sens. Actuators, B*, 2005, **107**, 53–58.
54 M. Shamsipur, T. Poursaberi, A. R. Karami, M. Hosseini, A. Momeni, N. Alizadeh, M. Yousefi and M. R. Ganjali, *Anal. Chim. Acta*, 2004, **501**, 55–60.
55 M. Ahmad and R. Narayanaswamy, *Sens. Actuators, B*, 2002, **81**, 259–266.
56 C. C. Li and M. S. Kuo, *Anal. Sci.*, 2002, **18**, 607–609.
57 M. R. Baezzat and M. Karimi, *Int. J. ChemTech Res.*, 2013, **5**, 2503–2507.
58 H. Tavallali and M. Yazdandoust, *Eurasian J. Anal. Chem.*, 2008, **3**, 284–287.
59 C. Sanchez-Pedreno, J. A. Ortuno, M. I. Albero, M. S. Garcia and M. V. Valero, *Anal. Chim. Acta*, 2000, **414**, 195–203.
60 C. Xiong, M. He and B. Hu, *Talanta*, 2008, **76**, 772–779.
61 H. Peng, N. Zhang, M. He, B. Chen and B. Hu, *Talanta*, 2015, **131**, 266–272.
62 Y. Zhang, B. Chen, S. Wu, M. He and B. Hu, *Talanta*, 2016, **154**, 474–480.
63 D. Mendil, Z. Demirci, O. D. Uluozlu, M. Tuzen and M. Soylak, *Food Chem.*, 2017, **221**, 1394–1399.
64 Y. Wang, J. Xie, Y. Wu, X. Hu, C. Yang and Q. Xu, *Talanta*, 2013, **112**, 123–128.
65 J. Ali, M. Tuzen, X. Feng and T. G. Kazi, *Food Chem.*, 2021, **344**, 128706.
66 A. N. Acikkapia, M. Tuzena and H. Baki, *Food Chem.*, 2019, **284**, 1–7.
67 L. A. Escudero, P. H. Pacheco, J. A. Gasquez and J. A. Salonia, *Food Chem.*, 2015, **169**, 73–79.
68 M. Atasoy and I. Kula, *Food Chem.*, 2022, **369**, 130938.
69 M. L. Chen and M. I. An, *Talanta*, 2012, **95**, 31–35.
70 A. S. Amin, *J. AOAC Int.*, 2014, **97**, 586–592.
71 J. N. Miller and J. C. Miller, *Statistics and Chemometrics for Analytical Chemistry*, Pearson/Prentice Hall, Harlow, UK, 5th edn, 2005, pp. 58–67.